Reliability Assessment of Multiple Quantum Well Avalanche Photodiodes

Ilgu Yun, Hicham M. Menkara*, Yang Wang, Ismail H. Oguzman, Jan Kolnik, Kevin F. Brennan, Gary S. May, Christopher J. Summers*, and Brent K. Wagner*

School of Electrical and Computer Engineering
*Georgia Tech Research Institute
Georgia Institute of Technology
Atlanta, GA 30332-0250

Abstract - The reliability of doped-barrier AlGaAs/GaAs multi-quantum well avalanche photodiodes fabricated by MBE is investigated via accelerated life tests. Dark current and breakdown voltage were the parameters monitored. The activation energy of the degradation mechanism and median device lifetime were determined. Device failure probability as a function of time was computed using the lognormal model. Analysis using the electron-beam induced current (EBIC) method revealed the degradation to be caused by ionic impurities or contamination in the passivation layer.

1.0 Introduction

Multiple quantum well avalanche photodiodes (APDs) are of interest as an ultra-low noise image capture mechanism for high definition systems [1]. In this application, the image capture stage must have sufficient optical gain to enable very sensitive light detection, but at the same time, the gain derived during detection must not contribute additional noise. Properly designed APDs can meet these specifications, but the long-term performance of these devices under conditions approximating actual operation is of critical importance in determining system reliability.

In this paper, accelerated life testing of AlGaAs/GaAs multiple quantum well (MQW) APDs has been conducted with the objective of estimating long-term device reliability. Since an increase in dark current results in a reduction of the APD signal-to-noise ratio [2] and breakdown voltage determines the operational voltage range of the device, these two factors represent the most sensitive indicators of the characteristic degradation in these devices. Thus, dark current and breakdown voltage were the parameters monitored in this study. The degradation in these parameters was investigated via high temperature storage tests and accelerated life tests, and the results of these tests were used to estimate device lifetime by assuming an Arrhenius-type temperature dependence [3]. Using the median device lifetime and its standard deviation as parameters, the failure probability of each device as a function of time was computed [4].

Following device stressing, analysis was conducted to determine the failure mechanism. It has been previously reported that the APD failure modes are primarily surface failures, such as electrode failure due to the interfacial reaction between metal and semiconductor or oxide contamination in the semiconductor surface [5-6]. High temperature operation will accelerate surface failures by increasing the mobility of the contaminants. Potential failure mechanisms were evaluated using scanning electron microscopy (SEM) and the electron-beam induced current (EBIC) method [7]. Based on this analysis, a failure mechanism of ionic impurities or contamination in the passivation layer at the junction perimeter is proposed.

2.0 Accelerated Life Testing

2.1 Device Structure and Fabrication

The device structure of the photodiodes investigated is shown in Figure 1. The devices were grown by molecular beam epitaxy (MBE) at the Georgia Tech Research Institute. The basic structure was that of a p-i-n diode where the intrinsic region was composed of the MQW superlattice structure. The p and n contact layers are 1.0 μm and 1.5 μm thick, respectively, and doped at a level of 10^{18} cm^{-3} [8]. The 1-3 μm thick GaAs/AlGaAs superlattice region consists of 25 periods of 200 Å GaAs quantum wells separated by 800 Å AlGaAs barrier layers. One complete period consists of a 300 Å high-field AlGaAs region doped at 3×10^{18} cm^{-3}, the 200 Å undoped GaAs layer, and a 500 Å undoped AlGaAs layer.

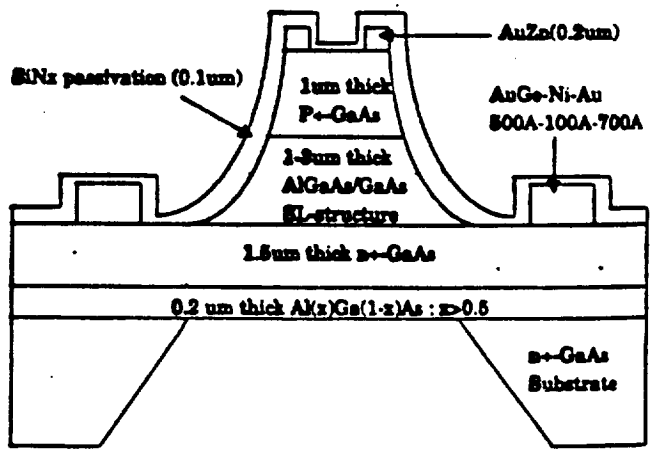

Figure 1 - Cross section of AlGaAs/GaAs MQW APD.

0-7803-2031-X/95/$4.00 © 1995 IEEE

The devices were fabricated on 2×10^{-4} cm^2 mesa structures with an active diameter in the range of 75-130 μm using standard photolithography techniques [9]. Since both p and n layers can be illuminated by removing the substrates, the device configuration allows for electron or hole injection [10]. A SiN_x passivation coating suppresses surface leakage current and provides the devices with very low dark currents.

2.2 Test Conditions

High temperature storage tests and accelerated life tests were performed on four different devices with a constant reverse current of 10 μA for 200 hours at three different ambient temperature levels: 100, 150 and 200°C. These conditions are summarized in Table I. The accelerated life tests measured the failure rate under stressful conditions (i.e. - a reverse bias voltage of approximately 7-9 V), the failure activation energy for the devices, and the average device lifetime. It was assumed that the temperature dependence of the failure rate (R) obeys the following Arrhenius law:

$$R = R_0 * \exp(-E_a/kT) \qquad (1)$$

where R_0 is a temperature-independent pre-exponential failure acceleration factor, E_a is the activation energy, T is the absolute temperature, and k is Boltzmann's constant. During these tests, dark current and breakdown voltage were measured at room temperature (25°C). The breakdown voltage was defined from the device I-V curve using the tangential line method. Typical breakdown voltages for these devices were in the range of 7.5-9 V. The APDs were classified as failing when the dark currents at room temperature and 90% of the breakdown voltage exceeded 1 μA.

Table I: Life Test Conditions

Temperature	Current	# Samples	Time
100°C	10 μA	4	200 hrs
150°C	10 μA	4	200 hrs
200°C	10 μA	4	200 hrs

3.0 Life Test Results

Several observations were made as a result of the accelerated life tests. First, dark current increases due to thermal overstress under bias were generally found to be exponentially dependent on the time of exposure to the reverse-bias electric field. This fact is shown Figure 3, in which the dark current at a given reverse-bias voltage increases significantly as a function of aging time. Breakdown voltage, on the other hand, was shown to be nearly linearly dependent on stressing time (Figure 4).

Figure 5 shows the percent of cumulative failures for the AlGaAs/GaAs APDs versus the lognormal projection of the device time-to-failure after accelerated life testing. In this representation, although the sample size is small, the data does indeed appear linear, which indicates that the failure mode is the wearout type, and

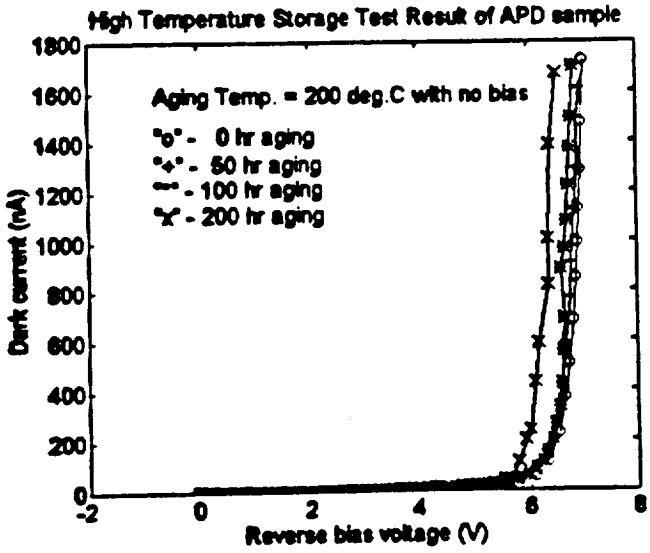

Figure 2 - Room-temperature I-V curve of an APD sample after 0, 50, 100, and 200 hours of unbiased baking at 200° C.

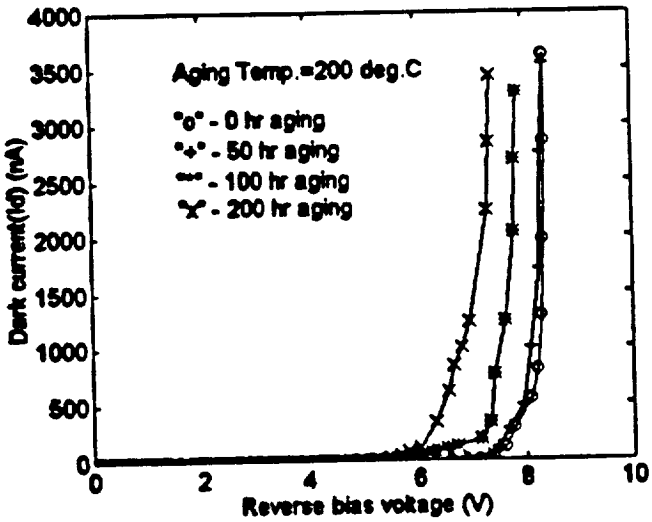

Figure 3 - Room-temperature I-V curve of an APD sample after 0, 50, 100, and 200 hours of aging under bias at 200° C.

failures obey the lognormal distribution relatively well [5]. Median lifetimes at 100, 150, and 200°C are estimated to be 1400, 210, and 70 hours, respectively, with a standard deviation of 1.81. A few test points exhibit slight deviation from linear behavior, but this may be attributed to the small sample size, as well as to infant mortality, since the deviations typically occur at the 25% level.

The Arrhenius plot of median lifetimes as a function of reciprocal aging temperature is shown in Figure 6. From this plot, the thermal activation energy of the device aging process is computed to be 0.46 eV [3]. Using this activation energy level, the median APD lifetime for all 16 samples under practical use conditions can be estimated to be 4.8×10^4 hours (approximately 5.5 years) at room temperature, with a standard devia-

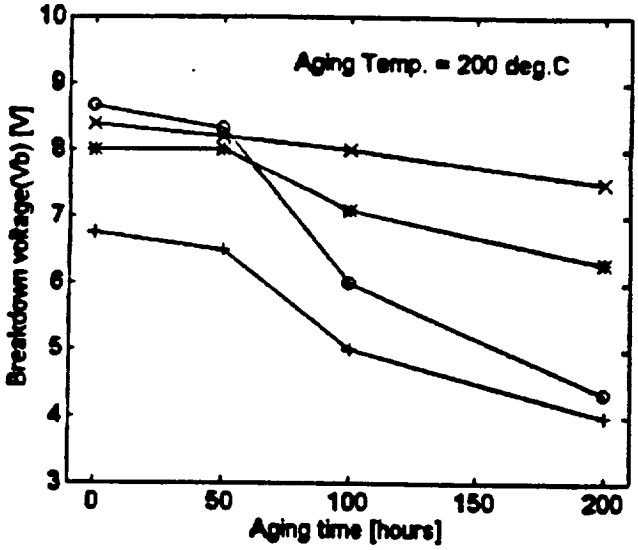

Figure 4 - Breakdown voltage variations after accelerated life testing at 200° C.

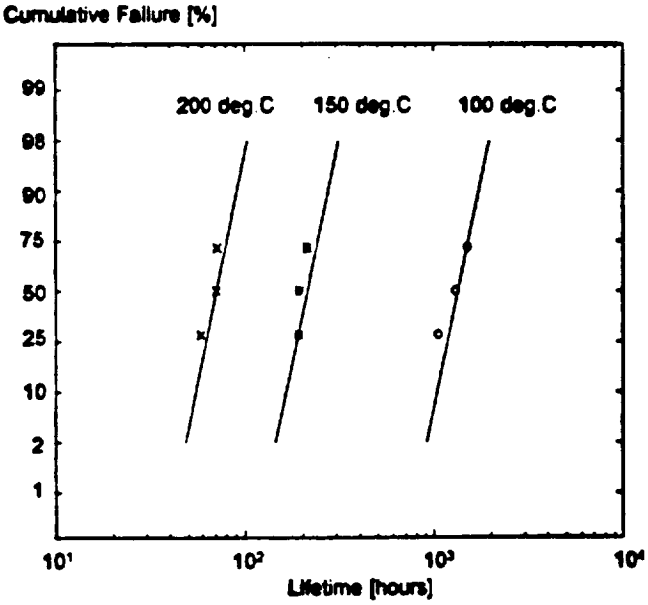

Figure 5 - Lognormal projection of time-to-failure versus percent of cumulative failures for the AlGaAs/GaAs APDs after life testing at 100, 150, and 200° C.

tion of 113 hours.

Due to the lognormal degradation behavior of the APDs, the failure probability of each device as a function of time, P(t), may be computed from the lognormal failure model by using the average device lifetime (μ) and its standard deviation (σ) as [4]:

$$P(t) = \frac{1}{\sigma\sqrt{2\pi}} \int_0^t \frac{1}{t} \exp\left[-\frac{(\ln t - \mu)^2}{2\sigma^2}\right] dt \qquad (2)$$

Along with Figure 5, this expression provides a quantitative method of evaluating the likelihood of failure for

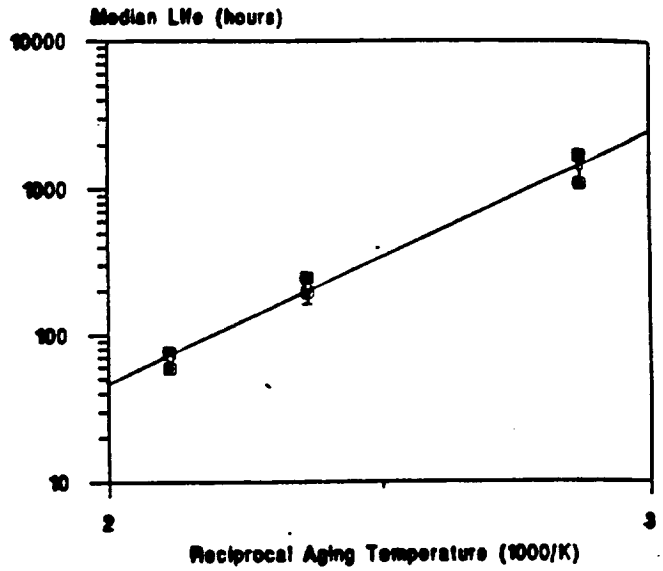

Figure 6 - Arrhenius plot of median device lifetimes as a function of reciprocal aging temperature.

a given device as a function of its age.

4.0 Failure Analysis and Discussion

Failure analysis on the thermally stressed devices was carried out using scanning electron microscopy (SEM) and the electron-beam induced current (EBIC) method [7]. Prior to this analysis, two possible causes for dark current increases were hypothesized: 1) the presence of contaminants in passivating nitrides at the junction; or 2) the degradation of the surface due to thermal and electrical overstress on the interface causing an increase of the surface component of dark current [11]. Figure 7 shows an SEM image of a device prior to life testing.

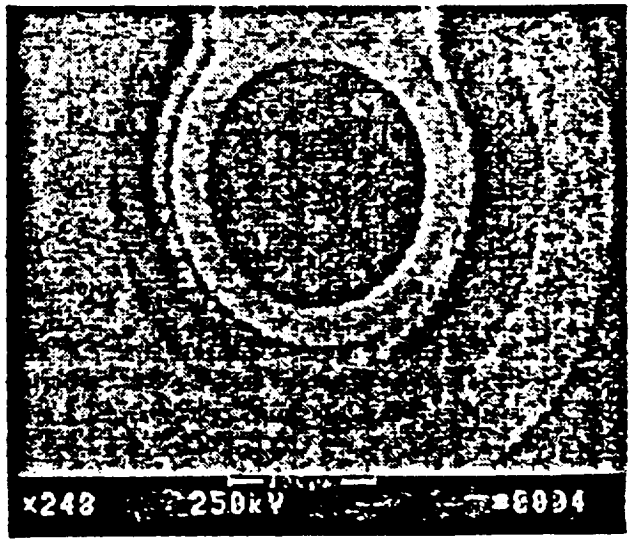

Figure 7 - SEM image of GaAs MQW APD before accelerated life testing.

From SEM and EBIC analysis of the degraded

samples, it was determined that the dark current increase was most likely due to the presence of ionic impurities or contamination in the silicon nitride passivation layer at the junction perimeter that generates a leakage path shorting the junction under the effect of electric field. This leakage is associated with low-resistance paths for carriers that consequently provide a mechanism for an increase in dark current. This hypothesis is supported by the fact that unbiased baking of the APD samples resulted in significantly less degradation, which is demonstrated by a comparison of Figures 2 and 3.

An example of surface contamination which causes a local leakage path shorting the pn junction appears in Figure 8. A common contaminant for silicon nitride passivating films is ionic sodium [12]. Efforts are presently underway to experimentally identify of the contaminant in this case. It has been suggested that these type of defects occur at metal-rich precipitates, some of which occur at crystal dislocations. The cause of the gradual reduction in breakdown voltage, on the other hand, is not known explicitly, but presumably involves the field-assisted and temperature-assisted drift of some impurity species or defects to localized sites in the pn junction.

5.0 Conclusion

Accelerated life tests of doped-barrier AlGaAs/GaAs MQW APDs were performed from the viewpoint of evaluating long-term reliability. From the life test results, the activation energy of the degradation mechanism was determined to be approximately 0.46 eV and the median lifetime of these devices was estimated to be 4.8×10^4 hours at room temperature. In addition, the failure probability of the devices was computed from the lognormal failure model by using the average lifetime and the standard deviation of that lifetime as parameters. Subsequent failure analysis using the SEM and EBIC methods clarified that the degradation due to dark current increase was brought about by the presence of ionic impurities or contamination in the passivation layer at the junction perimeter that generate a leakage path and shorts the junction under the effect of electric field.

In the near future, these life test results will be compared to other APD structures, including undoped and doped-well devices. These structures are all being considered as candidates for the high-definition system image capture application. The purpose of this comparison will be to determine the advantages and disadvantages of each device structure in terms of reliability.

Acknowledgement

The authors would like to thank NASA (contract no. NAGW-2753) for support of this research. We are also grateful to Alan Doolittle for his aid in performing EBIC experiments and for many helpful discussions.

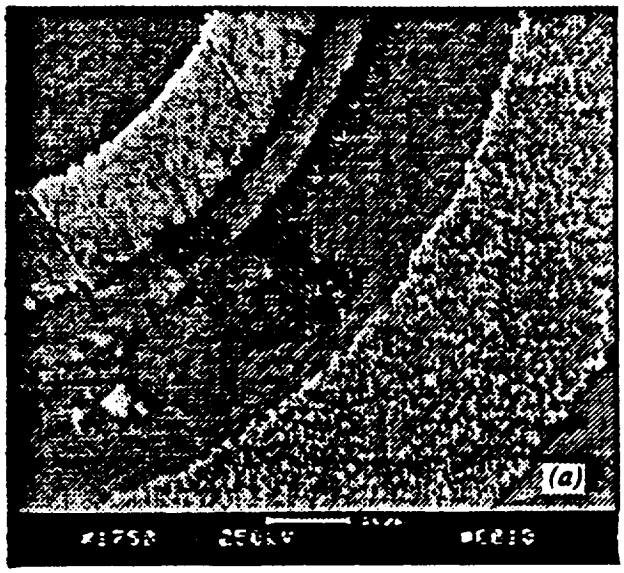

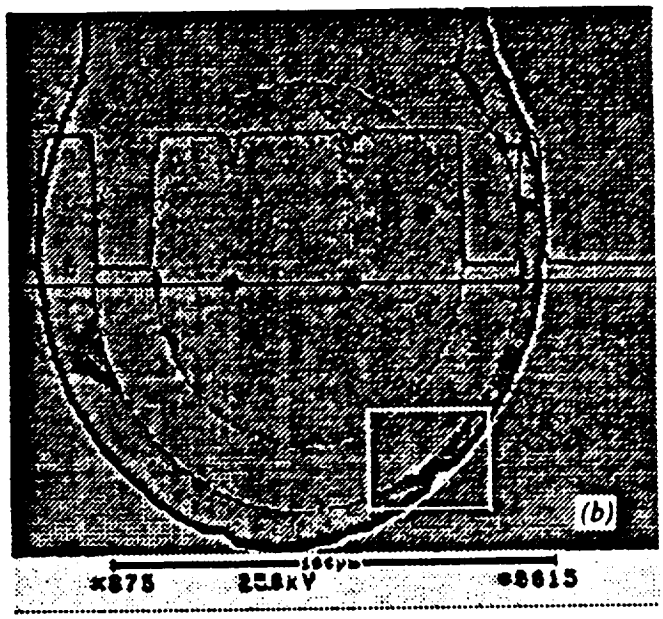

Figure 8 - (a) SEM and (b) EBIC images of GaAs MQW APD after accelerated life testing at 200° C.

References

[1] K. Brennan, "Theory of the Doped Quantum Well Superlattice APD: A New Solid State Photomultiplier," *IEEE J. Quan. Elec.*, vol. QE-22, pp. 1999-2016, 1986.

[2] M. Teich, K. Matsuo, and B. Saleh, "Excess Noise Factors for Conventional and Superlattice Avalanche Photodiodes and Photomultiplier Tubes," *IEEE J. Quan. Elec.*, vol. QE-22, pp. 1184-1193, 1987.

[3] W. Joyce, K. Liou, F. Nash, P. Bossard, and R. Hartman, "Methodology of Accelerated Aging", *AT&T Tech. Journal*, vol. 64, no. 3, pp. 717-764, March, 1985.

[4] F. Nash, *Estimating Device Reliability*, Boston: Kluwer, 1993.

[5] H. Sudo and M. Suzuki, "Surface Degradation Mechanism of InP/InGaAs APDs," *J. Lightwave Tech.*, vol. 6, no. 10, pp. 1496-1501, Oct., 1988.

[6] J. Bauer and R. Trommer, "Long-term Operation of Planar InGaAs/InP p-i-n Photodiodes," *IEEE Trans. Elec. Dev.*, vol. 35, no. 12, pp. 2349-2353, Dec., 1988.

[7] E. Pollino, *Microelectronic Reliability*, vol. 2, Boston: Artech House, 1989.

[8] P. Aristin, A. Torabi, A. Garrison, H. Harris and C. Summers, "Evaluation of New Multiple Quantum Well Avalanche Photodiode Structures: The MOW, The Doped Barrier and Doped Quantum Well," *Inst. Phys. Conf. Series*, no. 120, 1991.

[9] P. Aristin, A. Torabi, A. Garrison, H. Harris and C. Summers, "New Doped Multiple Quantum Well Avalanche Photodiode: The Doped Barrier $Al_{0.35}/Ga_{0.65}/As/GaAs$ Multiple Quantum Well Avalanche Photodiode", *Appl. Phys. Lett.*, vol. 60, no. 1, pp. 85-87, Jan., 1992.

[10] A. Torabi, K. Brennan, and C. Summers, "Growt and Application of Superlattices and Quantur Wells", *SPIE Proc.*, vol. 835, pp. 90-94, 1988.

[11] Y. Kuhara, H. Terauchi and H. Nishizawa, "Reli bility of InGaAs/InP Long-Wavelength p-i-n Photc diodes Passivated with Polyimide Thin Film", *Jou nal of Lightwave Tech.*, vol. LT-4, no. 7, pp. 93 936, July, 1986.

[12] S. Wolf and R. Tauber, *Silicon Processing for th VLSI Era*, Sunset Beach, CA: Lattice Press, 1986.

[13] H. Sudo, Y. Nakano and G. Iwane, "Reliability c Germanium Avalanche Photodiodes for Optic Transmission Systems", *IEEE Tran. Elec. Dev* vol. ED-33, no. 1, pp. 98-103, Jan., 1986

[14] C. Skrimshire, J. Farr, D. Sloan, M. Robertson, I Putland, J. Stokoe and R. Sutherland, "Reliabili of Mesa and Planar InGaAs PIN Photodiodes", *IE Proc.*, vol. 137, no. 1, pp. 74-78, Feb., 1990.